Geophysical Research Letters

Supporting Information for

New Inferences on Magma Dynamics in Melilitite-Carbonatite Volcanoes: The Case Study of Mt. Vulture (Southern Italy)

G. Carnevale[1], A. Caracausi[2], S. G. Rotolo[1,2], M. Paternoster[3], and V. Zanon[4]

[1] Dipartimento di Scienze della Terra e del Mare, Università degli Studi di Palermo, Palermo, Italy, [2] Istituto Nazionale di Geofisica e Vulcanologia, Sezione di Palermo, Palermo, Italy, [3] Dipartimento di Scienze, Università degli Studi della Basilicata, Potenza, Italy, [4] Instituto de Vulcanologia e Avaliação de Riscos, Universidade dos Açores, Ponta Delgada, Portugal

Contents of this file

Introduction

This supplementary information file includes a general description of the geological background of the Mt. Vulture and further details about petrography, mineral chemistry and fluid inclusions of the study samples, with also details about analytical methods and geometries of the pelletal lapilli. Figure S1 shows the core and the fine-grained mineral assemblage of the rim of the pelletal lapilli. Figure S2 shows diagrams of some geochemical tracers from Mt. Vulture loose clinopyroxene xenocrysts. Figure S3 shows diagrams of the main geometric characteristics of pelletal lapilli. Table S1 shows minerochemical composition of olivine from the core of pelletal lapilli and loose olivine xenocrysts. Table S2 shows minerochemical composition of clinopyroxene from the core of pelletal lapilli and loose clinopyroxene xenocrysts. Table S3 shows the micro-thermometric data. Table S4 shows the geometric parameters of pelletal lapilli.

Text S1.

Geological Background.

Mount Vulture is one of the major Quaternary volcanoes of the central Italian peninsula, located within Apulian foreland with a consistent east offset with respect to the peri-thyrrenian Campanian-Latium-Tuscany volcanic alignment. The Moho beneath the Mt. Vulture is around 32 km with a lithospheric thickness approaching 100 km (Kelemework et al., 2021; Peccerillo, 2017). Mt. Vulture volcano activity started at ca. 740 ka and continued until ca. 480 ka (Villa & Buettner, 2009). After a long period of quiescence, a small volume explosive eruption of carbonatite-melilitite magma at about 140 ka (Villa & Buettner, 2009) occurred, forming also two intra-caldera maars, now occupied by the Monticchio Lakes (D'Orazio et al., 2007; Stoppa & Principe, 1997).

The erupted silicate magmas are all silica undersaturated, ranging from foidites (leucitites, haünites, nephelinites), tephrites and basanites to phonolites (Peccerillo, 2017). The presence of intrusive calciocarbonatite ejecta (sövite), carbonatitic tephra in the pyroclastic products and carbonatite lava flows, witness the role of carbonatite magmatism beneath Mt. Vulture area (D'Orazio et al., 2007; Rosatelli et al., 2000; Stoppa & Principe, 1997), although the primary origin of the carbonate fraction is yet to be univocally accepted (D'Orazio et al., 2007, 2008; Stoppa et al., 2008).

The volcanic units of Mt. Vulture are divided into two Super-Synthems and five Synthems (Giannandrea et al., 2006). The Monticchio Lakes Synthem (MLS) represents the most recent activity of Vulture volcano and includes five Sub-Synthems, among which only Lago Piccolo is currently dated (132 ± 12 ka, Brocchini et al., 1994). Apparently, only three (Casa Rossa, Lago Piccolo and Serra di Braida) of the five Sub-Synthems of the MLS are characterised by the presence of abundant lapilli, ultramafic mantle xenoliths and mafic xenocrysts, described in depth for their petrographic and geochemical characterization (Downes et al., 2002; Jones et al., 2000; Rosatelli et al., 2007; Stoppa & Principe, 1997). They consist essentially of unaltered spinel-lherzolite, harzburgites, dunites, wehrlite and clinopyroxenites (Downes et al., 2002; Jones et al., 2000). Geothermobarometric studies (En-Sp and Di-Sp thermo-barometers) constrained pressures and temperatures in the range of 1.4-2.2 GPa and 1050-1150 °C respectively (Jones et al., 2000).

Petrography and Mineral Chemistry.

The ultramafic cores of studied pelletal lapilli consist essentially of olivine and clinopyroxene phenocrysts with very rare orthopyroxene (wherlites), while few samples are characterised only by olivine megacrysts (dunites).

Olivine from the ultramafic cores of pelletal lapilli usually shows irregular elongated shape with curvilinear boundaries and also undulose extinction and intracrystalline deformation structures (see Figure 2 in the main text). Inclusions of spinel in olivine phenocrysts are also present. Clinopyroxene occurs as a distinctive emerald green coloured Cr-diopside and it occurs in all of the samples subhedral/anhedral with strongly curvilinear boundaries, apparently with no deformation structures.

Cr_2O_3 content of olivine from the ultramafic cores of pelletal lapilli and of loose olivine xenocrysts varies in a very narrow range from 0.02 to 0.04 wt.% (Table S1).

SiO_2 and CaO content of clinopyroxene from the ultramafic core of pelletal lapilli ranges from 51.7 to 53.1 wt.% and from 22.2 to 22.9 wt.% respectively, while SiO_2 and CaO content in loose clinopyroxene xenocrysts ranges from 52.2 to 54.6 wt.% and from 20.1 to 22.7 wt.% respectively. The Mg# values are uniformly high, and they range from 0.90 to 0.92 (in ultramafic cores) and from 0.89 to 0.91 (in loose xenocrysts). TiO_2 and Al_2O_3 content is low and ranges from 0.15 to 0.5 wt.% (in both ultramafic cores and loose xenocrysts) and from 3.6 to 4 wt.% (in ultramafic cores) and 2 to 5.5 wt.% (in loose xenocrysts), respectively (Table S2). The rim of ultramafic core of pelletal lapilli is composed of fine-grained micro-phenocrysts of häuyne, with xenocrystic debris of olivine and clinopyroxene (Figure S1).

Literature data refer of some crystal chemical and geochemical patterns in clinopyroxene such as the Ca/Al ratio, $^{87}Sr/^{86}Sr$ ratio and also Mg#, as possible tracers of carbonatite mantle metasomatism (Zong & Liu, 2018). If plotted in Ca/Al vs Mg# and $^{87}Sr/^{86}Sr$ vs Ca/Al diagrams, clinopyroxenes present as loose xenocrysts and in the Mt. Vulture xenoliths fall into the mantle-related carbonate metasomatism field (Figure S2). Indeed, clinopyroxenes from Mt. Vulture show restricted range of every ratio ($5 \leq Ca/Al \leq 14$; $0.88 \leq Mg\# \leq 0.91$; $0.70424 \leq {^{87}Sr}/{^{86}Sr} \leq 0.70585$) (data from Downes et al., 2002; Jones et al., 2000), in accordance with type 2 mantle-related carbonate metasomatism described by Zong and Liu (2018).

Fluid Inclusions.

We analysed 171 fluid inclusions in loose xenocrysts of olivine, 107 in clinopyroxene (Cr-diopside), and 184 fluid inclusions in the ultramafic cores of studied lapilli (68 in olivine and 116 Cr-diopside) (Table S3), all being <10 μm in size and most of them in the range of 1-5 μm.

In loose xenocrysts, secondary fluid inclusions (distinguished on the basis of their textural characteristics and distribution within the crystals) are more abundant than primary fluid inclusions and tend to be smaller than the primary ones. On the contrary, in olivine and Cr-diopside in the ultramafic cores of pelletal lapilli, early stage fluid inclusions are more abundant than late stage fluid inclusions.

Trapping pressures and densities were estimated at the trapping temperature of 1100 °C, an intermediate temperature value of the temperature range (1050-1150 °C) previously calculated by Jones et al. (2000) with En-Sp and Di-Sp thermo-barometers. Finally, in order to convert barometric data into depths, we made some assumptions on crustal density of along the inferred magma pathway, using the stratigraphy presented in the CROP-4 deep seismic profile beneath the Mt. Vulture area (Scrocca et al., 2007). Considering (i) the average value of 2600 kg/m^3 of the shallow crust lithologies, (ii) an average value of 3300 kg/m^3 of the shallow mantle lithologies, and (iii) the probable presence of a mafic body beneath Mt. Vulture (Improta et al., 2014 and references therein), a single representative average value of 3000 kg/m^3 was considered.

Analytical Methods

Mineral composition of analysed samples was determined by a CAMECA SX100 electron microprobe at Observatoire des Sciences de l'Univers (UPMC-INSU) (Paris, France), operating at 15 kV accelerating voltage and a 20nA beam current.

Fluid Inclusions were studied in doubly-polished wafers and single mineral grains by a Linkam THMSG 600 microscopic heating/cooling stage, at the Instituto de Vulcanologia e Avaliação de Riscos (IVAR) (Ponta Delgada, Portugal). Loose xenocrysts samples of olivine and clinopyroxene were embedded in epoxy resin and doubly polished until a thickness of 100-80 μm. The stage was cooled with liquid nitrogen and calibrated using a single standard crystal of quartz with pure H_2O and CO_2 inclusions. Cooling and heating rates varied during the analysis. Indeed, in order to minimize the effect of metastable transformations during cooling, very common in fluid inclusions, melting and homogenization temperatures were determined during heating at the minimum rate (1 °C/min). For CO_2-rich inclusions (H_2O:CO_2 ratio = 1:10) densities were firstly calculated on the basis of the equation provided in Sterner and Bodnar (1991) and finally corrected according to Hansteen and Klügel (2008), while isochore trajectories/curves were calculated using the software "Fluids" (Bakker, 2003).

Geometric Parameters of Pelletal Lapilli.

In order to calculate all aspect ratio-related parameters of pelletal lapilli (i.e. major and minor axis, perimeter, cross-sectional area of rim and core and circularity values), individual samples were selected, digitised and processed in the image-analysis software package ImageJ, following the method of Gernon et al. (2012). The main geometric measurements of pelletal lapilli are reported in Table S4. The minimum axis of the entire pelletal lapilli sample data set range from 6.4 to 14 mm, while the maximum axis ranges from 6.9 to 16.1 mm. As regards the ultramafic cores of lapilli, the minimum axis ranges from 2.5 to 8.8 mm and the maximum axis ranges from 4.8 to 10 mm. The calculated cross-sectional areas of rims of pelletal lapilli show a good correlation with cross-sectional areas of cores (Figure S3), with a correlation coefficient r = 0.84. The circularity (defined as 4π x area/perimeter^2) varies from 0.4 to 1.0 (*i.e.* 1.0 indicates a perfect circle), although the percentage frequency distribution shows that the most frequent value is 0.8 (Figure S3).

Pelletal lapilli associated with diatreme-maar systems present similar physical and geometrical characteristics to specific particles formed during an industrial process known as fluidised spray granulation process, widely used in industrial engineering and applied in geological contexts in some explosive eruptions (e.g., Gernon et al., 2012). The observed geometrical characteristics of Mt. Vulture pelletal lapilli (see Table S4) are similar to those of southern African ones associated with volcaniclastic kimberlite of Venetia and Letšeng (Gernon et al., 2012). Indeed, considering the evaluation of the aspect ratio and internal structure of both pelletal lapilli occurrences, they show moderate to strong positive correlation between the cross-sectional areas of rims and cores, with high circularity values (Figure S3), suggesting a uniform process of coating.

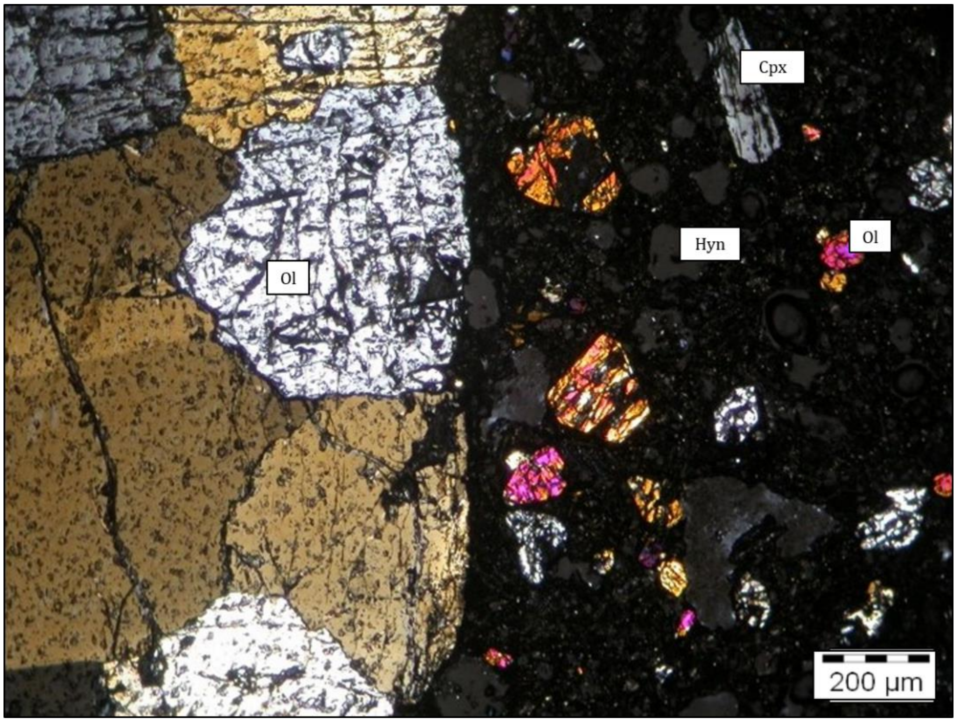

Figure S1. Crossed polars microphotograph showing the olivine micro-phenocrysts of the wehrlitic core of pelletal lapilli (on the left) and the rim of pelletal lapilli composed of fine-grained micro-phenocrysts of häuyne and xenocrystic debris of olivine and clinopyroxene (on the right), Monticchio Lake Synthem, Mt. Vulture volcano.

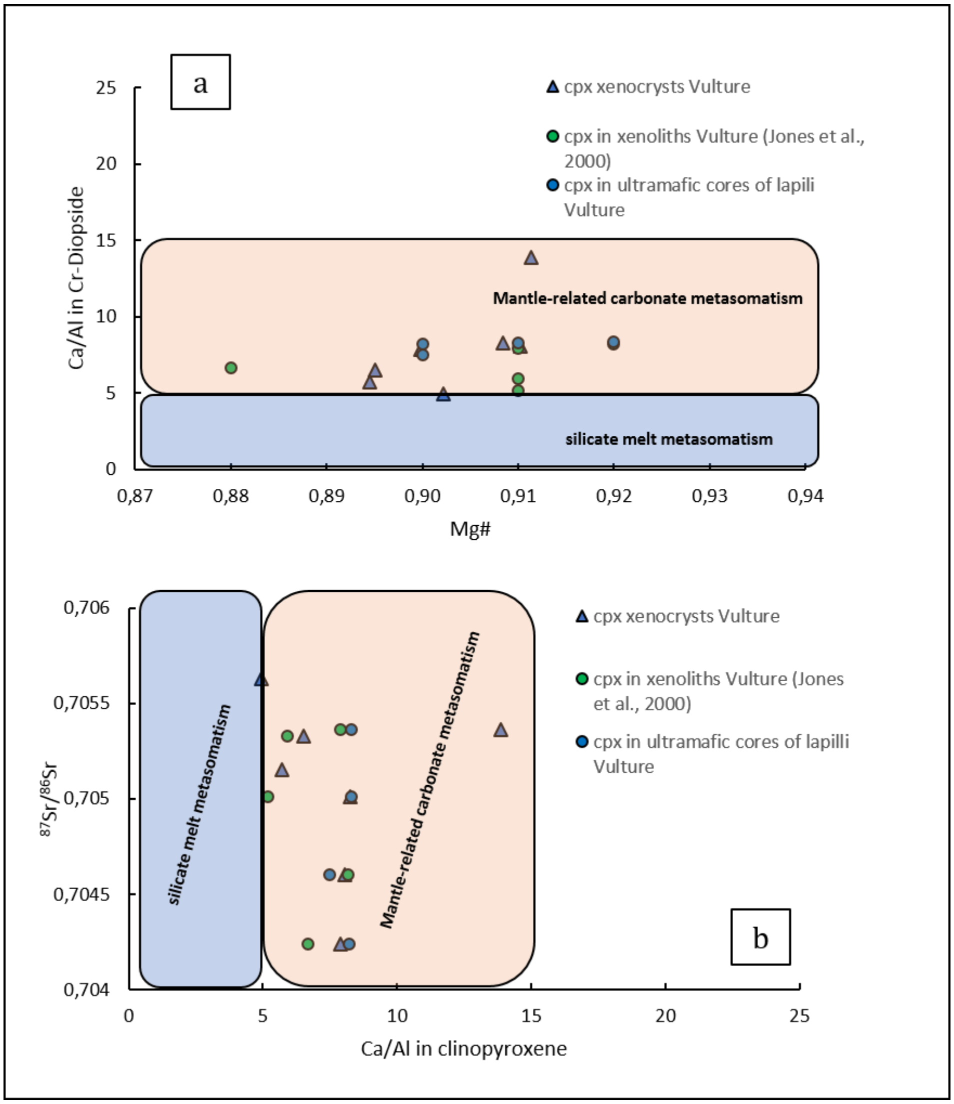

Figure S2. Ca/Al ratio vs. a) Mg# and b) $^{87}Sr/^{86}Sr$ ratio of clinopyroxene from Mt. Vulture. Sr isotopic ratios are from Downes et al. (2002). Fields of carbonate vs. silicate melts metasomatism are taken from Zong and Liu (2018).

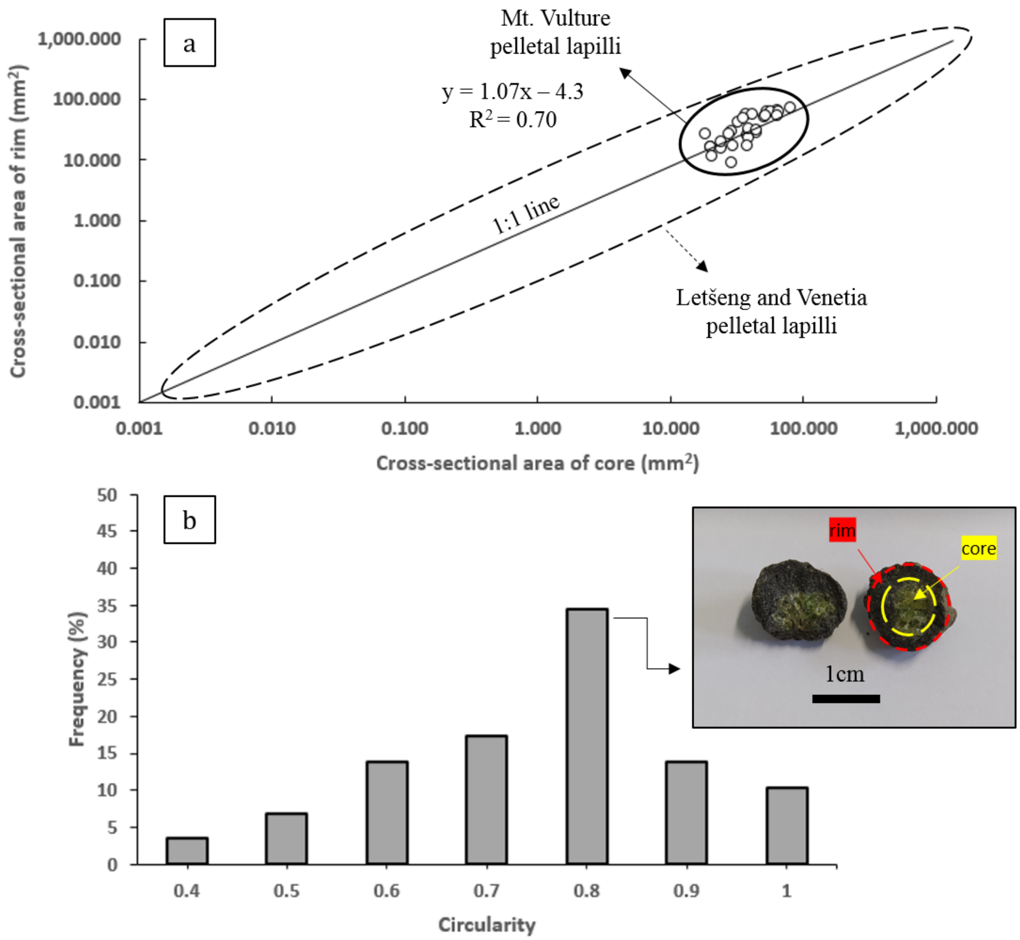

Figure S3. Diagrams of the main geometric characteristics of pelletal lapilli from Mt. Vulture. a) Cross-sectional area of core vs. cross-sectional area of rim (data of pelletal lapilli from Letšeng and Venetia are also plotted for comparison; Gernon et al., 2012). b) Histograms showing circularity values of pelletal lapilli.

Table S1. Minerochemical composition of olivine from the core of pelletal lapilli and loose olivine xenocrysts from Vulture volcano, Monticchio Lakes Synthem.

Sample	ol-lap1	ol-lap2	ol-lap3	ol-lap4	ol-lap5	ol-lap6	ol-lap7
	core	core	core	core	core	core	core
SiO_2 (wt. %)	41.73	41.70	41.97	42.04	40.76	40.66	40.22
$FeO_{tot.}$	8.97	9.15	9.02	8.97	9.03	10.07	9.00
MnO	0.14	0.14	0.14	0.14	0.13	0.16	0.14
MgO	49.62	49.79	49.66	49.71	50.09	50.80	51.48
CaO	0.09	0.09	0.08	0.09	0.09	0.10	0.09
Cr_2O_3	0.03	0.03	0.03	0.03	0.03	0.03	0.03

NiO	0.38	0.37	0.38	0.37	0.39	0.35	0.37
Tot.	100.95	101.27	101.28	101.35	100.52	102.16	101.33
Mg#	0.91	0.91	0.91	0.91	0.91	0.90	0.91
Fo	90.79	90.65	90.75	90.81	90.82	90.00	91.07
Fa	9.21	9.35	9.25	9.19	9.18	10.00	8.93

Notes: Mg# = (Mg/Mg + Fe). Each reported analysis is the mean of three spots and core-rim analyses do not show significant zonation.

Table S1. Cont.

Sample	ol-xeno1	ol-xeno2	ol-xeno3	ol-xeno4	ol-xeno5	ol-xeno6	ol-xeno7
	xenocryst	xenocryst	xenocryst	xenocryst	xenocryst	xenocryst	xenocryst
SiO_2 (wt. %)	40.50	39.65	40.56	41.50	40.09	41.67	40.97
$FeO_{tot.}$	9.36	10.35	8.11	9.66	9.06	8.49	10.11
MnO	0.14	0.15	0.11	0.13	0.12	0.11	0.14
MgO	49.87	48.97	50.75	50.72	49.83	49.60	50.32
CaO	0.15	0.14	0.19	0.18	0.12	0.18	0.14
Cr_2O_3	0.03	0.02	0.04	0.02	0.04	0.03	0.02
NiO	0.38	0.37	0.41	0.37	0.40	0.39	0.37
Tot.	100.43	99.64	100.16	102.59	99.66	100.48	102.07
Mg#	0.90	0.89	0.92	0.90	0.91	0.91	0.90
Fo	90.48	89.40	91.78	90.35	90.75	91.24	89.87
Fa	9.52	10.60	8.22	9.65	9.25	8.76	10.13

Notes: Mg# = (Mg/Mg + Fe). Each reported analysis is the mean of three spots and core-rim analyses do not show significant zonation.

Table S2. Minerochemical composition of clinopyroxene from the core of pelletal lapilli and loose clinopyroxene xenocrysts from Vulture volcano, Monticchio Lakes Synthem.

Sample	Cr-di lap1	Cr-di lap2	Cr-di lap3	Cr-di lap4
	core	core	core	core
SiO_2 (wt. %)	52.3039	52.9848	53.1418	51.7559
TiO_2	0.33	0.40	0.15	0.48
Al_2O_3	3.63	3.72	3.68	4.02
FeO	2.78	2.59	3.13	3.40
MnO	0.00	0.00	0.00	0.00
MgO	16.20	16.55	16.40	16.44

CaO	22.29	22.90	22.40	22.24
Na_2O	0.62	0.56	0.52	0.49
Cr_2O_3	1.35	1.31	1.47	1.29
Tot.	99.50	101.01	100.89	100.12
Mg#	0.91	0.92	0.90	0.90
Wo	47.42	47.76	46.99	46.57
En	47.96	48.02	47.88	47.88
Fs	4.62	4.22	5.13	5.55

Notes: Mg# = (Mg/Mg + Fe). Each reported analysis is the mean of three spots and core-rim analyses do not show significant zonation.

Table S2. Cont.

Sample	Cr-di1	Cr-di2	Cr-di3	Cr-di4	Cr-di5	Cr-di6	Cr-di7
	xenocryst	xenocryst	xenocryst	xenocryst	xenocryst	xenocryst	xenocryst
SiO_2 (wt. %)	54.56	53.09	52.91	52.81	53.13	52.46	52.19
TiO_2	0.16	0.31	0.37	0.38	0.43	0.14	0.48
Al_2O_3	2.09	3.67	3.84	3.80	4.55	5.48	5.19
FeO	3.02	2.90	3.20	2.91	3.33	3.20	3.42
MnO	0.00	0.00	0.00	0.00	0.00	0.00	0.00
MgO	17.42	16.12	16.12	16.52	15.91	16.55	16.25
CaO	21.43	22.41	22.38	22.71	21.91	20.15	21.98
Na_2O	0.73	0.64	0.71	0.61	0.75	1.10	0.79
Cr_2O_3	1.15	1.28	0.92	0.93	0.42	1.25	0.86
Tot.	100.55	100.42	100.45	100.67	100.42	100.33	101.16
Mg#	0.91	0.91	0.90	0.91	0.90	0.90	0.89
Wo	44.62	47.58	47.31	47.34	46.97	44.12	46.51
En	50.47	47.62	47.42	47.93	47.47	50.42	47.84
Fs	4.91	4.80	5.28	4.73	5.56	5.47	5.64

Notes: Mg# = (Mg/Mg + Fe). Each reported analysis is the mean of three spots and core-rim analyses do not show significant zonation.

Table S3. Micro-thermometric data of studied samples.

Sample	**Mineral analysed**	**N° measures**	**Th (°C)**	**ρ (g/cm^3)**	**ρ (g/cm^3)$_{corrected}$**
Ol-I	olivine (5)	46	Th_L 11.5 – 30.2	0.58 – 0.85	0.61 – 0.89
Ol-II	olivine (1)	12	Th_L 13.0 – 20.9	0.76 – 0.84	0.80 – 0.88

Ol-III	olivine (2)	113	Th_L 23.3 – 30.9	0.52 – 0.73	0.54 – 0.77
Cr-cpx I	clinopyroxene (2)	77	Th_L 2.7 – 13.2	0.84 – 0.91	0.88 – 0.95
Cr-cpx II	clinopyroxene (1)	30	Th_L -20.0 – -15.1	1.01 – 1.03	1.05 – 1.08
LAP-1	olivine (1)	40	Th_L -27.7 – -23.4	1.05 – 1.07	1.10 – 1.11
	clinopyroxene (2)	36	Th_L -27.3 – -8.5	0.98 – 1.06	1.02 – 1.11
LAP-2	olivine (1)	28	Th_L -9.0 – 30.3	0.58 – 0.98	0.60 – 1.02
	clinopyroxene (1)	80	Th_L -13.5 – -11.5	0.99 – 1.00	1.04 – 1.05

Notes: in brackets the number of analysed minerals; Th= homogenization temperature; ρ = density

Table S4. Calculated geometric parameters of studied pelletal lapilli from Vulture volcano, Monticchio Lakes Synthem.

Sample	**ax_{min}** (mm)	**ax_{max}**	**ax $core_{min}$**	**ax $core_{max}$**	**P** (mm)	**P core**	**A** (mm^2)	**A core**	**A rim**	**circularity**
LAP-1W	14.0	15.0	7.5	10.0	47.1	31.4	153.9	78.5	75.4	0.9
LAP-2W	13.0	15.8	6.7	9.0	49.6	28.3	132.7	63.6	69.1	0.7
LAP-3W	11.4	14.7	7.9	8.0	46.2	25.1	102.0	50.2	51.8	0.6
LAP-4W	8.7	9.7	3.7	6.0	30.5	18.8	59.4	28.3	31.2	0.8
LAP-5W	7.1	8.2	4.1	5.5	25.7	17.3	39.6	23.7	15.8	0.7
LAP-6W	9.7	11.9	7.0	7.5	37.4	23.6	73.9	44.2	29.7	0.7
LAP-7W	9.8	12.5	3.8	6.4	39.3	20.1	75.4	32.2	43.2	0.6
LAP-8W	12.2	14.9	4.0	8.2	46.8	25.7	116.8	52.8	64.1	0.7
LAP-9W	12.5	14.0	6.0	8.5	44.0	26.7	122.7	56.7	65.9	0.8
LAP-10W	11.0	16.1	2.5	6.8	50.6	21.4	95.0	36.3	58.7	0.5
LAP-11ol	9.3	10.3	6.6	7.0	32.3	22.0	67.9	38.5	29.4	0.8
LAP-12ol	12.8	14.5	8.8	9.1	45.5	28.6	128.6	65.0	63.6	0.8
LAP-13D	12.3	12.4	5.0	9.0	38.9	28.3	118.8	63.6	55.2	1.0
LAP-14ol	9.0	10.6	6.5	6.9	33.3	21.7	63.6	37.4	26.2	0.7
LAP-15D	11.3	11.4	5.9	7.2	35.8	22.6	100.2	40.7	59.5	1.0
LAP-16ol	8.9	10.0	4.1	7.0	31.4	22.0	62.2	38.5	23.7	0.8
LAP-17W	9.6	9.7	6.8	7.0	30.5	22.0	72.3	38.5	33.9	1.0
LAP-18W	6.8	7.5	3.9	5.0	23.6	15.7	36.3	19.6	16.7	0.8
LAP-19W	7.7	8.8	5.8	6.1	27.6	19.2	46.5	29.2	17.3	0.8
LAP-20D	6.9	10.5	5.7	6.0	33.0	18.8	37.4	28.3	9.1	0.4
LAP-21W	6.8	7.3	4.5	5.0	22.9	15.7	36.3	19.6	16.7	0.9
LAP-22D	7.6	10.0	4.7	4.8	31.4	15.1	45.3	18.1	27.3	0.6
LAP-23D	8.4	11.0	4.6	5.9	34.5	18.5	55.4	27.3	28.1	0.6
LAP-24W	6.4	6.9	5.0	5.1	21.7	16.0	32.2	20.4	11.7	0.9
LAP-25W	8.4	9.2	6.8	6.9	28.9	21.7	55.4	37.4	18.0	0.8
LAP-26W	9.9	10.7	6.8	7.5	33.6	23.6	76.9	44.2	32.8	0.9
LAP-27D	11.7	12.8	7.0	8.1	40.2	25.4	107.5	51.5	56.0	0.8
LAP-28W	7.5	10.6	5.3	5.5	33.3	17.3	44.2	23.7	20.4	0.5
LAP-29W	10.4	11.3	5.5	6.7	35.5	21.0	84.9	35.2	49.7	0.8

Notes: W = wehrlite; D = dunite; ol = olivine; ax = axis; P = perimeter; A = area.

References.

Bakker, R. J. (2003). Package FLUIDS 1. Computer programs for analysis of fluid inclusion data and for modelling bulk fluid properties. *Chemical Geology*, *194*(1–3), 3–23. https://doi.org/10.1016/S0009-2541(02)00268-1

Brocchini, D., La Volpe, L., Laurenzi, M. A., & Principe, C. (1994). Storia evolutiva del Monte Vulture. *Plinius*, *12*, 22–25.

D'Orazio, M., Innocenti, F., Tonarini, S., & Doglioni, C. (2007). Carbonatites in a subduction system: The Pleistocene alvikites from Mt. Vulture (southern Italy). *Lithos*, *98*(1–4), 313–334. https://doi.org/10.1016/j.lithos.2007.05.004

D'Orazio, M., Innocenti, F., Tonarini, S., & Doglioni, C. (2008). Reply to the discussion of: "Carbonatites in a subduction system: The Pleistocene alvikites from Mt. Vulture (Southern Italy)" by M. D'Orazio, F. Innocenti, S. Tonarini and C. Doglioni (Lithos 98, 313-334) by F. Stoppa, C. Principe and P. Giannandrea. *Lithos*, *103*(3–4), 557–561. https://doi.org/10.1016/j.lithos.2007.10.010

Downes, H., Kostoula, T., Jones, A. P., Beard, A. D., Thirlwall, M. F., & Bodinier, J. L. (2002). Geochemistry and Sr-Nd isotopic compositions of mantle xenoliths from the Monte Vulture carbonatite-melilitite volcano, central southern Italy. *Contributions to Mineralogy and Petrology*, *144*(1), 78–92. https://doi.org/10.1007/s00410-002-0383-4

Gernon, T. M., Brown, R. J., Tait, M. A., & Hincks, T. K. (2012). The origin of pelletal lapilli in explosive kimberlite eruptions. *Nature Communications*, *3*(May), 832–837. https://doi.org/10.1038/ncomms1842

Giannandrea, P., La Volpe, L., Principe, C., & Schiattarella, M. (2006). Unità stratigrafiche a limiti inconformi e storia evolutiva del vulcano medio-pleistocenico di Monte Vulture (Appennino meridionale, Italia). *Bollettino Della Societa Geologica Italiana*, *125*(1), 67–92.

Hansteen, T. H., & Klügel, A. (2008). Fluid inclusion thermobarometry as a tracer for magmatic processes. *Reviews in Mineralogy and Geochemistry*, *69*(Roedder 1984), 143–177. https://doi.org/10.2138/rmg.2008.69.5

Improta, L., De Gori, P., & Chiarabba, C. (2014). New insights into crustal structure, Cenozoic magmatism, CO2 degassing, and seismogenesis in the southern Apennines and Irpinia region from local earthquake tomography. *Journal of Geophysical Research: Solid Earth*, *119*(11), 8283–8311. https://doi.org/10.1002/2013JB010890

Jones, A. P., Kostoula, T., Stoppa, F., & Woolley, A. R. (2000). Petrography and mineral chemistry of mantle xenoliths in a carbonate-rich melilititic tuff from Mt. Vulture volcano, southern Italy. *Mineralogical Magazine*, *64*(4), 593–613.

https://doi.org/10.1180/002646100549634

Kelemework, Y., Milano, M., La Manna, M., de Alteriis, G., Iorio, M., & Fedi, M. (2021). Crustal structure in the Campanian region (Southern Apennines, Italy) from potential field modelling. *Scientific Reports*, *11*(1), 1–18. https://doi.org/10.1038/s41598-021-93945-8

Peccerillo, A. (2017). The Apulian Province (Mount Vulture). *Advances in Volcanology*, 203–216. https://doi.org/10.1007/978-3-319-42491-0_8

Rosatelli, G., Stoppa, F., & Jones, A. P. (2000). Intrusive calcite-carbonatite occurrence from Mt. Vulture volcano, southern Italy. *Mineralogical Magazine*, *64*(4), 615–624. https://doi.org/10.1180/002646100549643

Rosatelli, G., Wall, F., & Stoppa, F. (2007). Calcio-carbonatite melts and metasomatism in the mantle beneath Mt. Vulture (Southern Italy). *Lithos*, *99*(3–4), 229–248. https://doi.org/10.1016/j.lithos.2007.05.011

Scrocca, D., Sciamanna, S., Di Luzio, E., Tozi, M., Nicolai, C., & Gambini, R. (2007). Structural setting along the CROP-04 deep seismic profile (Southern Apennines - Italy). *Bollettino Della Societa Geologica Italiana, Supplemento*, *7*(February 2007), 283–296.

Sterner, S. M., & Bodnar, R. J. (1991). Synthetic fluid inclusions. X: Experimental determination of P-V-T-X properties in the CO2-H2O system to 6 kb and 700 °C. *American Journal of Science*, *291*, 1–54. https://doi.org/https://doi.org/10.2475/ajs.291.1.1

Stoppa, F., Principe, C., & Giannandrea, P. (2008). Comments on: Carbonatites in a subduction system: The Pleistocene alvikites from Mt. Vulture (southern Italy) by d'Orazio et al., (2007). *Lithos*, *103*(3–4), 550–556. https://doi.org/10.1016/j.lithos.2007.10.012

Stoppa, F., & Principe, C. (1997). Eruption style and petrology of a new carbonatitic suite from the Mt. Vulture Southern Italy /: The Monticchio Lakes Formation. *Journal of Volcanology and Geothermal Research*, *78*(3–4), 251–265. https://doi.org/10.1016/S0377-0273(97)00004-8

Villa, I. M., & Buettner, A. (2009). Chronostratigraphy of Monte Vulture volcano (southern Italy): Secondary mineral microtextures and 39Ar-40Ar systematics. *Bulletin of Volcanology*, *71*(10), 1195–1208. https://doi.org/10.1007/s00445-009-0294-6

Zong, K., & Liu, Y. (2018). Carbonate metasomatism in the lithospheric mantle: Implications for cratonic destruction in North China. *Science China Earth Sciences*, *61*(6), 711–729. https://doi.org/10.1007/s11430-017-9185-2